INTERNATIONAL JOURNAL FOR NUMERICAL METHODS IN ENGINEERING, VOL. 39, 2005–2029 (1996)

HYPERSINGULAR RESIDUALS—A NEW APPROACH FOR ERROR ESTIMATION IN THE BOUNDARY ELEMENT METHOD

GLAUCIO H. PAULINO

School of Civil and Environmental Engineering, Cornell University, Ithaca, NY 14853, U.S.A.

L. J. GRAY

Mathematical Sciences Section, Computer Science and Mathematics Division, Oak Ridge National Laboratory, Oak Ridge, TN 37831, U.S.A.

VREJ ZARIKIAN

Department of Mathematics, University of Central Florida, Orlando, FL 32816, U.S.A.

SUMMARY

This paper presents a new approach for *a posteriori* 'pointwise' error estimation in the boundary element method. The estimator relies upon evaluation of the residual of hypersingular integral equations, and is therefore intrinsic to the boundary integral equation approach. A methodology is developed for approximating the error on the boundary as well as in the interior of the domain. Extensive computational experiments have been performed for the two-dimensional Laplace equation and the numerical results indicate that the error estimates successfully track the form of the exact error curve. Moreover, a reasonable estimate of the magnitude of the actual error is also predicted.

KEY WORDS: residual estimates; singular and hypersingular residuals; error estimates; boundary element method; singular integrals; hypersingular integrals

1. INTRODUCTION

Whenever a numerical method is utilized to solve the governing differential equations of a problem, error is introduced by the discretization process which reduces the continuous mathematical model to one having a finite number of degrees of freedom. The discretization errors are defined as the difference between the actual solution of the differential equation and its numerical approximation. Reliable estimation of these errors is essential to guarantee a certain level of accuracy of the numerical solution, and is a key component of adaptive procedures. Estimation of the discretization error in the Boundary Element Method (BEM) is the focus of this work. Other types of errors, such as roundoff errors and uncertainties in material, geometry and boundary conditions are not considered in this work.

There are several recent surveys of the literature on error estimation and adaptivity, and the reader is directed to the appropriate references. Kita and Kamiya[1] have reviewed some of the recent studies on error estimation and adaptive mesh refinement in the BEM. The volumes edited

CCC 0029–5981/96/122005–25

Received 6 June 1995
Revised 21 August 1995

by Brebbia and Aliabadi[2] and by Babuška *et al.*[3] review adaptive techniques for the Finite Element Method (FEM) and the BEM. Recent surveys of the literature in FEM include the articles by Noor and Babuška,[4] Oden and Demkowicz,[5] Strouboulis and Haque,[6,7] and Babuška and Suri.[8] Mackerle[9] has presented a bibliography on mesh generation and refinement for FEM and BEM published from 1990 to 1993. The volume edited by Babůska *et al.*[10] presents adaptive techniques for the FEM and the Finite Difference Method (FDM). A general *a posteriori* error estimation method, which can be applied to the FEM, BEM, and FDM has been presented by Kelly *et al.*[11] The above references indicate the importance of the field of error estimation and adaptivity in the numerical analysis of partial differential equations.

Recent textbooks in the FEM emphasize the field of adaptive solution techniques. The book by Zienkiewicz and Taylor[12] includes a chapter on 'error estimation and adaptivity' (Chapter 14), which can be supplemented by References.[13-15] The recent book by Szabó and Babuška[16] is primarily concerned with this subject. Due to the importance of this topic, textbooks on the BEM will likely follow the same trend.

Quite naturally, the BEM literature on error estimation and adaptivity shows a significant influence of the FEM. Although it is certainly possible to benefit from the FEM technology, a simple translation of concepts from one method to the other may not be the most appropriate. Guiggiani[17] has commented that more attention should be devoted to techniques intrinsic to the BEM, and within this spirit, the method proposed herein is rooted in the boundary integral methodology.

A simple local error estimate of the residual type, based upon hypersingular integral equations, is introduced in this paper. These equations have proven to be highly useful in a variety of situations, and their definition and numerical evaluation are now well understood (see, for example, Gray,[18] Gray *et al.*,[19] Gray and Manne,[20] Krishnasamy *et al.*,[21] Guiggiani *et al.*,[22] Rosen and Cormack[23,24]). The measure of the error on the boundary of a body is taken as the amount by which the solution to the standard Boundary Integral Equation (BIE) fails to satisfy the equally valid hypersingular BIE. Distinctive advantages of this approach are that the estimator does not require boundary values away from the nodal points, it does not involve any adjustable parameters, it is defined by an analytical formula, and it is intrinsic to the BEM. This allows the derivation of a relationship between the exact and estimated (here the residual) errors, and provides a natural extension of the procedure to interior error estimates. It is worth mentioning that, despite its importance, interior error estimation has not received attention in the BEM literature. Furthermore, a primary goal of this paper is to present extensive test calculations which validate the error method and provide a reasonable basis for claiming that the proposed error estimates are reliable and will perform well in most situations.

The remaining sections of this paper are organized as follows. First, the basic BIEs are given, and the method for estimating the local error on the boundary is presented, including the derivation of a relationship between the exact and the estimated (residual) errors. Next, the method for interior estimates is developed. This includes error estimates for both the function (e.g. potential) and its derivatives. Subsequent to the theoretical part of this work, a few aspects concerning the computational implementation are discussed, and numerical examples comparing the exact and estimated errors are presented. Afterwards, conclusions are stated and promising directions for future research are discussed. The Appendix presents the formulation for evaluating discretization errors in elasticity problems.

2. LOCAL ERROR ESTIMATES

A method for *a posteriori* 'pointwise' evaluation of the error on the boundary, ∂B, and in the interior, B, of the domain $\Omega = B \cup \partial B$ is presented in this section. The error is 'pointwise' in the

sense that it can be evaluated at selected points of the boundary or interior of the domain. For interior error estimation, the formulation is developed for both the field variable and its derivatives (e.g. potential and interior gradients for potential problems). For simplicity, the error estimates will be defined in the context of the two-dimensional Laplace equation $\nabla^2\phi = 0$. However, the method is general, and applicable to any boundary integral formulation (see Appendix).

2.1. *Boundary integral equations*

For simplicity, the subscript notation

$$\phi_{\mathbf{D}} \equiv \frac{\partial}{\partial \mathbf{D}}\phi \quad \text{and} \quad \phi_{\mathbf{d}} \equiv \frac{\partial}{\partial \mathbf{d}}\phi$$

will be employed for directional derivatives, with the upper/lower case letters utilized to distinguish differentiation with respect to the collocation point P and the field point Q (integration variable), respectively, in a BIE. Here, $\mathbf{D}$ and $\mathbf{d}$ refer to generic unit direction vectors, and ϕ denotes the potential.

With the above notation, the boundary integral formulation for the two-dimensional Laplace equation can be written as

$$\phi(P) + \int_{\partial B} \phi(Q)\frac{\partial}{\partial \mathbf{n}}G(P,Q)\,\mathrm{d}s_Q = \int_{\partial B} \phi_{\mathbf{n}}(Q)G(P,Q)\,\mathrm{d}s_Q \tag{1}$$

where $\phi_{\mathbf{n}}$ is the boundary flux (normal derivative of ϕ), $\mathrm{d}s$ denotes a differential length element, and the Green's function is taken as the point source potential

$$G(P,Q) = -\frac{1}{2\pi}\log\|Q - P\| \tag{2}$$

Equation (1) is valid for points P in the interior B (thus the coefficient 1 for the leading term). However, as discussed by Lutz and Gray,[25] it is also valid for P on the boundary, provided the singular integrals are defined as a *limit-to-the-boundary*. Let ∂B_{d} and ∂B_{n} denote the portions of the boundary having Dirichlet (ϕ prescribed) and Neumann ($\phi_{\mathbf{n}}$ prescribed) boundary conditions, respectively. Thus, equation (1) can be employed to solve for the unknowns ϕ on ∂B_{n} and $\phi_{\mathbf{n}}$ on ∂B_{d}, and $\partial B = \partial B_{\mathrm{d}} + \partial B_{\mathrm{n}}$.

For $P \in B$, the integrands in equation (1) are not singular, and the derivative of this equation with respect to P can be computed by interchanging the order of differentiation and integration. The resulting gradient BIE can therefore be expressed as

$$(\nabla\phi\cdot\mathbf{D})(P) + \int_{\partial B} \phi(Q)\nabla\frac{\partial}{\partial \mathbf{n}}G(P,Q)\cdot\mathbf{D}\,\mathrm{d}s_Q = \int_{\partial B} \phi_{\mathbf{n}}(Q)\nabla G(P,Q)\cdot\mathbf{D}\,\mathrm{d}s_Q \tag{3}$$

where $\mathbf{D} = (D_1, D_2)$ is any specified unit direction vector. Once again, a well defined integral equation on the boundary, $P \in \partial B$, results by defining the singular integrals as a *limit* in which P approaches ∂B.[18,26]

2.2. *Boundary error estimate*

Assume now that a particular problem has been solved using equation (1), resulting in approximate solutions

$$\tilde{\phi} \quad \text{and} \quad \tilde{\phi}_{\mathbf{n}}$$

for the unknown boundary values of potential and flux, respectively. These approximate solutions, together with the specified boundary conditions, determine these boundary functions on the approximate geometry. Although these functions have been determined to satisfy equation (1), in whatever sense this equation was approximated (e.g. collocation, Galerkin), these values are not necessarily consistent with equation (3).

The proposed error estimate $\mathscr{E}(P)$ is defined as the residual which arises when the approximate solution is substituted into equation (3), i.e. $\mathscr{E}(P)$ is the *hypersingular residual*. Thus,

$$\mathscr{E}(P) = -\tilde{\phi}_{\mathbf{D}}(P) - \int_{\widetilde{\partial B}} \tilde{\phi}(Q) \frac{\partial}{\partial \mathbf{D}} \frac{\partial}{\partial \mathbf{n}} G(P,Q)\, ds_Q + \int_{\widetilde{\partial B}} \tilde{\phi}_{\mathbf{n}}(Q) \frac{\partial}{\partial \mathbf{D}} G(P,Q)\, ds_Q \tag{4}$$

where $\widetilde{\partial B}$ represents the approximated boundary geometry. Therefore, $\mathscr{E}(P)$ is quite simply the amount by which the solution to the standard BIE (equation (1)) fails to satisfy the hypersingular BIE (equation (3)). The estimator $\mathscr{E}(P)$ is 'pointwise' in the sense that it can evaluated at selected boundary points, rather than everywhere. The specific choice of the vector $\mathbf{D}$ in equation (4) will be given later in this paper.

The estimator could have been defined with the sign reversed. The decision to employ equation (4) has been guided by the results of computational experiments with the interior error estimates (see Section 4). Moreover, if the boundary error estimates are to be used for a self-adaptive mesh refinement procedure, an appropriate error norm is generally used in the refinement process (e.g. References 16 and 27). In this case, only the magnitude of the local error is needed.

Note that residual and error are clearly different quantities, i.e. residual is not error. However, this work suggests, and presents computational evidence, that the residual of the hypersingular equation is a reasonable estimate of error in the boundary integral solution. The estimator defined by equation (4) does not require boundary values away from the nodal points, it does not involve adjustable parameters, it is defined by an analytical formula, and it is intrinsic to the BEM. These properties are important for the derivations presented in the remainder of this paper.

2.2.1. Relationship between the exact error and the hypersingular residual. A relationship between the exact errors and the hypersingular residual of equation (4) is presented here. If $\phi(Q)$ and $\phi_{\mathbf{n}}(Q)$ represent the exact solution, equation (3) is valid everywhere on ∂B and can be rewritten as

$$0 = -\phi_{\mathbf{D}}(P) - \int_{\partial B} \phi(Q) \frac{\partial}{\partial \mathbf{D}} \frac{\partial}{\partial \mathbf{n}} G(P,Q)\, ds_Q + \int_{\partial B} \phi_{\mathbf{n}}(Q) \frac{\partial}{\partial \mathbf{D}} G(P,Q)\, ds_Q \tag{5}$$

Subtracting this equation from equation (4), one obtains

$$\mathscr{E}(P) = -[\phi_{\mathbf{D}} - \tilde{\phi}_{\mathbf{D}}](P) - \int_{\partial B} [\phi - \tilde{\phi}](Q) \frac{\partial}{\partial \mathbf{D}} \frac{\partial}{\partial \mathbf{n}} G(P,Q)\, ds_Q + \int_{\partial B} [\phi_{\mathbf{n}} - \tilde{\phi}_{\mathbf{n}}](Q) \frac{\partial}{\partial \mathbf{D}} G(P,Q)\, ds_Q \tag{6}$$

where the error in approximating the geometry has been neglected in the present analysis (i.e. it is assumed that $\partial B \equiv \widetilde{\partial B}$). Defining the notation

$$\begin{aligned} E_{\phi_{\mathbf{D}}}(P) &= [\phi_{\mathbf{D}} - \tilde{\phi}_{\mathbf{D}}](P) \\ E_{\phi}(Q) &= [\phi - \tilde{\phi}](Q) \\ E_{\phi_{\mathbf{n}}}(Q) &= [\phi_{\mathbf{n}} - \tilde{\phi}_{\mathbf{n}}](Q) \end{aligned} \tag{7}$$

for the exact errors, one obtains

$$\mathscr{E}(P) = -E_{\phi_D}(P) - \int_{\partial B} E_{\phi}(Q) \frac{\partial}{\partial \mathbf{D}} \frac{\partial}{\partial \mathbf{n}} G(P,Q)\, ds_Q + \int_{\partial B} E_{\phi_n}(Q) \frac{\partial}{\partial \mathbf{D}} G(P,Q)\, ds_Q \tag{8}$$

At this point, this equation is presented to simply observe that there is a relationship between the exact error E and the residual function $\mathscr{E}$ on the boundary. However, it is hoped that further analytical or numerical development of this approach can exploit equation (8).

2.3. *Interior error estimates*

Interior error estimation is a subject that has not received attention in the BEM literature. Assessment of the interior error is important to investigate the behaviour of field variables, especially in the neighbourhood of corners, kinks, or locations with high boundary curvature. Moreover, it may have important applications in at least two areas of non-linear BEM analysis, the Dual Reciprocity Method (DRM) and material non-linearities. The DRM has been applied to a range of non-linear problems (see, for example, the book by Partridge *et al.*[28]). This method leads to a formulation involving boundary integrals only, however, interior nodal points are also included in the formulation. Therefore, error estimation for the DRM should involve both boundary and interior error estimates.

Wei *et al.*[29] have recently performed elasto-viscoplastic shape optimization of two-dimensional solids by the BEM. They have stated that 'the choice of mesh, especially the internal cells, is crucial for the solution of this class of problems. The best approach is to use adaptive meshing during the iterative optimization process'. Therefore, numerical analysis of materially non-linear problems by the BEM (for further information, see the book by Chandra and Mukherjee[30]) is a field where interior error estimation is of fundamental importance. In this case, domain integrals must also be added in the error formulation.

As will be demonstrated by the numerical examples in Section 4, $\mathscr{E}(P)$ provides an estimation of the error *everywhere* on the boundary. As a consequence, it is possible to develop an interior error estimate based upon the boundary error estimates. This formulation is developed below, and error estimates are presented for both the potential ϕ and its directional derivatives ϕ_D.

2.3.1. Error Estimate for $\phi(P)$, $P \in B$. For an interior point $P \in B$, the exact solution satisfies

$$\phi(P) = -\int_{\partial B} \phi(Q) \frac{\partial}{\partial \mathbf{n}} G(P,Q)\, ds_Q + \int_{\partial B} \phi_n(Q)\, G(P,Q)\, ds_Q \tag{9}$$

whereas the approximate solution at P is given by

$$\tilde{\phi}(P) = -\int_{\widetilde{\partial B}} \tilde{\phi}(Q) \frac{\partial}{\partial \mathbf{n}} G(P,Q)\, ds_Q + \int_{\widetilde{\partial B}} \tilde{\phi}_n(Q)\, G(P,Q)\, ds_Q \tag{10}$$

the boundary values $\tilde{\phi}(Q)$ and $\tilde{\phi}_n(Q)$ having been computed. Subtraction of equation (10) from equation (9) gives

$$[\phi - \tilde{\phi}](P) = -\int_{\partial B} [\phi - \tilde{\phi}](Q) \frac{\partial}{\partial \mathbf{n}} G(P,Q)\, ds_Q + \int_{\partial B} [\phi_n - \tilde{\phi}_n](Q)\, G(P,Q)\, ds_Q \tag{11}$$

where, as before, the error in approximating the geometry has been neglected. To obtain an estimate of the error at P, replace the exact errors (between square brackets) on the boundary by

the estimated values,

$$[\phi - \tilde{\phi}](Q) \approx \mathscr{E}_{\phi}(Q)$$
$$[\phi_n - \tilde{\phi}_n](Q) \approx \mathscr{E}_{\phi_n}(Q) \tag{12}$$

For Dirichlet portions of the boundary, $\mathscr{E}_{\phi_n} \equiv \mathscr{E}(Q)$, and *assume* (see Remark 3 in Section 2.4)

$$\mathscr{E}_{\phi}(Q) \equiv 0 \tag{13}$$

Similarly, for Neumann portions of the boundary, $\mathscr{E}_{\phi}(Q) \equiv \mathscr{E}(Q)$, and *assume*

$$\mathscr{E}_{\phi_n}(Q) \equiv 0 \tag{14}$$

Substituting equations (12) in equation (11), one obtains

$$\mathscr{E}_{\phi}(P) = -\int_{\partial B} \mathscr{E}_{\phi}(Q) \frac{\partial}{\partial \mathbf{n}} G(P,Q)\, ds_Q + \int_{\partial B} \mathscr{E}_{\phi_n}(Q)\, G(P,Q)\, ds_Q \tag{15}$$

where

$$\mathscr{E}_{\phi}(P) \approx [\phi - \tilde{\phi}](P) \tag{16}$$

As all quantities on the right-hand side of equation (15) are known, $\mathscr{E}_{\phi}(P)$ can be calculated.

2.3.2. Error Estimate for $\phi_D(P)$, $P \in B$. Equation (11) is the starting point for the derivation of an expression for $\mathscr{E}_{\phi_D}(P)$. Differentiating equation (11) with respect to $\mathbf{D}$ ($\|\mathbf{D}\| = 1$), one obtains

$$[\phi_D - \tilde{\phi}_D](P) = -\int_{\partial B} [\phi - \tilde{\phi}](Q) \frac{\partial}{\partial \mathbf{D}} \frac{\partial}{\partial \mathbf{n}} G(P,Q)\, ds_Q + \int_{\partial B} [\phi_n - \tilde{\phi}_n](Q) \frac{\partial}{\partial \mathbf{D}} G(P,Q)\, ds_Q \tag{17}$$

As before (Section 2.3.1), the exact errors (between square brackets) on the boundary are approximated by the estimated ones, and thus the error estimate for the directional derivatives of the potential at P is given by

$$\mathscr{E}_{\phi_D}(P) = -\int_{\partial B} \mathscr{E}_{\phi}(Q) \frac{\partial}{\partial \mathbf{D}} \frac{\partial}{\partial \mathbf{n}} G(P,Q)\, ds_Q + \int_{\partial B} \mathscr{E}_{\phi_n}(Q) \frac{\partial}{\partial \mathbf{D}} G(P,Q)\, ds_Q \tag{18}$$

where

$$\mathscr{E}_{\phi_D}(P) \approx [\phi_D - \tilde{\phi}_D](P) \tag{19}$$

Again, all the quantities on the right-hand side of equation (18) are known and $\mathscr{E}_{\phi_D}(P)$ can be calculated.

2.4. Remarks

Of the five remarks presented below, the first three concern characteristics relevant to the proposed *a posteriori* error estimates. The fourth remark points out the differences between the proposed hypersingular residual (see equations (4) and (8)) and the literature on residual type error estimates. The last remark discusses differences between this work and a previous error estimation technique which relies on hypersingular integral equations.

Remark 1 (Directional derivatives in the hypersingular BIEs). The vector **D** in equations (3) and (4) has not been specified yet. One would like to choose a direction **D** for which the error estimate $\mathscr{E}$ best tracks the exact error in the problem. Computational tests, involving two-dimensional problems, have been performed with both

$$\mathbf{D} \equiv \mathbf{N} \quad \text{and} \quad \mathbf{D} \equiv \mathbf{T}$$

where **N** and **T** denote the normal and tangential unit vectors, respectively, on the boundary ∂B at the source point P. Our tests indicate that using $\mathbf{D} \equiv \mathbf{N}$ in equation (4) provides more reliable error estimates than using $\mathbf{D} \equiv \mathbf{T}$.[31] However, the use of $\mathbf{D} \equiv \mathbf{T}$ in equation (4) might be useful in other situations, such as fracture mechanics problems (see Section 6).

An advantage of the error method presented here is that it can be readily extended to three-dimensional problems. Note that the functional form of the error equations remain the same, i.e. equations (4), (15) and (18) hold for both two- and three-dimensional problems. For three-dimensional problems, using equation (4) with the directional derivatives taken normal to the boundary is simpler and more efficient than using this equation with the directional derivatives taken tangent to the boundary. The former alternative requires one evaluation of equation (4) while the latter requires two evaluations of this equation.

Remark 2 ('Symmetry' of the method with respect to equations (1) *and* (3)). The argument which led to equation (4) is symmetric, i.e. if the hypersingular integral equation is used to solve the boundary value problem,[32] then the standard BEM equation can be used for error estimation. In other words, with respect to the error estimation method, equations (1) and (3) are complementary to each other. This is illustrated by Figure 1.

Specifically, assume that a particular problem has been solved using equation (3), resulting in approximate solutions $\tilde{\phi}$ and $\tilde{\phi}_{\mathbf{n}}$. The error estimate $\mathscr{E}(P)$ is now defined as the residual which arises when the approximate solution is substituted into equation (1), i.e. $\mathscr{E}(P)$ is the *singular residual.* Thus,

$$\mathscr{E}(P) = -\tilde{\phi}(P) - \int_{\widetilde{\partial B}} \tilde{\phi}(Q) \frac{\partial}{\partial \mathbf{n}} G(P,Q)\, \mathrm{d}s_Q + \int_{\widetilde{\partial B}} \tilde{\phi}_{\mathbf{n}}(Q)\, G(P,Q)\, \mathrm{d}s_Q \tag{20}$$

Similar to equation (4), the sign in equation (20) is also arbitrary. For the error in the interior, equations analogous to (15) and (18) can be readily obtained.

This 'symmetry' property is also important and necessary for estimating the error in the Symmetric-Galerkin BEM (e.g. see References 33 and 34). This approach potentially combines the accuracy of the Galerkin method with the speed of collocation calculations.[35] In this method, both the standard and the hypersingular BIEs are employed, the choice being dictated by the prescribed boundary condition. Thus, the ability to interchange the role of the two equations is essential for applying the error estimation approach to this new, and potentially important, approximation method. Test error estimation calculations using the Symmetric-Galerkin BEM are in progress.

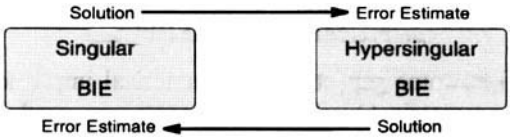

Figure 1. Interchange of equations (1) and (3)

Remark 3 (*Continuity to the boundary*). The formulation for the interior error estimates, presented in Section 2.3, is not continuous to the boundary. Continuity at the boundary is clearly a desirable property, and at the expense of additional computation, is achievable. The basic idea is to take $\mathscr{E}_\phi$ on ∂B_n and $\mathscr{E}_{\phi_n}$ on ∂B_d, obtained from equation (4), as 'boundary conditions' to equation (1), thereby solving for $\mathscr{E}_\phi$ on ∂B_d and $\mathscr{E}_{\phi_n}$ on ∂B_n, rather than assuming that they are zero. This procedure will lead to a set of boundary errors which provide a continuous limit to the boundary of the interior errors. Although the assumptions of zero error, equations (13) and (14), are reasonable, they are of an heuristic nature and do not have theoretical justification. The reason for first examining the method as described above is that it requires less computational effort, and will probably suffice for most applications.

Remark 4 (*Residual estimates*). Due to the lack of rigorous mathematical results, most work on error estimates for the BEM, including the present one, is based on heuristic approaches. There are some theoretical papers, which attempt to relate error and residual, e.g. References 36–38, but the results are only valid under particular circumstances.

Previous publications in residual type error estimates in the BEM include References 27 and 39–41. Parreira and Dong[27] and Rank[39] have estimated the residual at collocation points which are distinct from those of the initial analysis. Sun and Zamani[40] and Abe[41] have derived a relationship between the residual and the error from the BIE. However, the hypersingular residual (equation (4)), or the relationship between the exact errors and the hypersingular residual (equation (8)) have not appeared in any of the papers cited above. Since these papers do not consider hypersingular integrals, equations (4) and (8), or anything like them, cannot have appeared in any of the previous publications.

Remark 5 (*Related work*). An error indicator which also relies upon the ability to evaluate hypersingular integrals was recently proposed by Ingber and Mitra.[42] The approach suggested in the present paper, for evaluation of the error on the boundary, is therefore related to that discussed by these authors, but there is a fundamental difference in the two techniques. The idea motivating the procedure by Ingber and Mitra[42] is to measure the discrepancy between the imposed boundary conditions and the boundary element solution. They define the Error Indicator EI(j) for a boundary element ∂B_j as

$$\mathrm{EI(j)} = \begin{cases} \left\{ \int_{\partial B_j} [\phi - \tilde{\phi}]^2 \, \mathrm{d}s \right\}^{1/2} & \partial B_j \in \partial B_d \\ \left\{ \int_{\partial B_j} [\phi_n - \tilde{\phi}_n]^2 \, \mathrm{d}s \right\}^{1/2} & \partial B_j \in \partial B_n \end{cases} \tag{21}$$

As discussed above, the indicator $\mathscr{E}(P)$ proposed herein (equation (4)) is the hypersingular residual, i.e. the amount by which the solution to the standard boundary integral equation fails to satisfy the hypersingular integral equation. While equation (21) requires less computational work than equation (4), Ingber and Mitra[42] have not presented any justification for their procedure. Moreover, it does not appear that their error method can be extended in a natural fashion into the interior.

3. NUMERICAL ASPECTS

This section briefly describes some aspects of the numerical implementation employed in the computational tests. Isoparametric Overhauser elements are used in the approximation of equations (1) and (3). For the standard BEM, these cubic elements provide a higher-order approximation than the traditional linear and quadratic elements (e.g. Reference 43). For the

hypersingular BEM, the Overhauser approximation provides the required smoothness of the density functions at the collocation points, i.e. ϕ is $C^{1,\alpha}$ (Hölder continous). For a discussion of continuity requirements for density functions in the BEM, see Krishnasamy *et al.*[44] and Paulino[45].

In two dimensions, the Overhauser element utilizes four consecutive boundary nodes, $\{S_k\}_{k=1}^4$, to define the interval between the second and third nodes $[S_2, S_3]$. The explicit parametric form is

$$Q(t) = \left(\sum_{k=1}^{4} N_k(t)\, x_k, \sum_{k=1}^{4} N_k(t)\, y_k \right) \tag{22}$$

where $t \in [0, 1]$ and $S_k = (x_k, y_k)$ are the co-ordinates of the four points defining the element. The shape functions $N_k (k = 1, \ldots, 4)$ are

$$\begin{aligned} N_1(t) &= -(t - 2t^2 + t^3)/2 \\ N_2(t) &= (2 - 5t^2 + 3t^3)/2 \\ N_3(t) &= (t + 4t^2 - 3t^3)/2 \\ N_4(t) &= -(t^2 - t^3)/2 \end{aligned} \tag{23}$$

As indicated above, Overhauser elements are used in the discretization of both potential and flux in equations (1) and (3). For example, the corresponding isoparametric approximation for ϕ, denoted by $\Phi(t)$ is then

$$\Phi(t) = \sum_{i=1}^{4} N_k(t)\, \phi(S_k) \tag{24}$$

It is a straightforward exercise to verify that the approximations for $Q(t)$ and ϕ are differentiable everywhere on the boundary.

Corners have been handled here by a 'double node' approach. It consists of defining one of the endpoint nodes (e.g. $k = 1$) and its adjacent node (e.g. $k = 2$) at the same location on the Overhauser element. At this location, the element does not provide C^1 continuity for the boundary geometry and the functional representation. The other endpoint of the element maintains the continuity conditions provided it is connected with another Overhauser element.

Two integration techniques have been employed here: numerical and analytical. Numerical integrations, evaluated with four point Gauss quadrature, have been employed for non-singular integrals. Analytical integrations have been used to compute the singular integrals. These integrals have been regularized by means of the *limit-to-the-boundary* definition.[26] Paulino[45] discusses in detail this regularization procedure.

Note that if $\mathbf{D} \equiv \mathbf{N} \equiv \mathbf{n}(P)$, then all quantities on the right-hand side of equation (4) are known, and $\mathscr{E}(P)$ can be readily calculated. If $\mathbf{D} \neq \mathbf{N}$, then the first term on the right-hand side of equation (4) can be obtained by differentiating the shape functions to compute the required tangential derivatives. Further information on the numerical scheme adopted here can be found in Reference 45.

4. COMPUTATIONAL RESULTS

A primary goal of this paper is to examine, by means of computational experiments, the performance of the new error estimates. Numerical results have been obtained for the two-dimensional Laplace equation on interior domains, employing Dirichlet and mixed boundary conditions. Additional examples can be found in References 31 and 46.

In order to assess various features of the proposed error estimates, the following examples are presented:

(1) Dirichlet problems
  (1.1) Circle
  (1.2) Ellipse
(2) Mixed boundary conditions
  (2.1) Simple modelling
  (2.2) 'Double node' modelling for change in boundary conditions
(3) Interior error estimates
  (3.1) Error for $\phi(P)$, $P \in B$
  (3.2) Error for $\phi_{\mathbf{D}}(P)$, $P \in B$
(4) Verification of the 'symmetry' of the method with respect to equations (1) and (3)
(5) Generic example: L-shaped domain

For all but the last calculation, the problems possess a simple analytical solution, allowing a comparison between the exact and estimated errors. The potential field is specified as

$$\phi(x, y) = \Re(z^4) = x^4 - 6x^2y^2 + y^4 \tag{25}$$

where $z = x + iy$, $i = \sqrt{-1}$, and $\Re$ denotes the real part of the complex function. As the goal with this procedure is to assess the accuracy of the proposed error estimates, *a fourth-order potential field is employed to ensure that the Overhauser cubics introduce error.* The corresponding gradient of the potential in equation (25) is

$$\nabla\phi(x, y) = (4x^3 - 12xy^2, 4y^3 - 12x^2y) \tag{26}$$

Unless otherwise stated, $\mathbf{D} \equiv \mathbf{N}$ has been used for the error estimate in equation (4), and the meshes for the elliptical geometries, $x^2/a^2 + y^2/b^2 = 1$, have been discretized with equal ellipse parameter angles. This discretization procedure is likely to introduce more error variation over the boundary than using a discretization with equal arc length. The last example represents a more practical problem geometry and boundary conditions for which there is no analytical solution available.

4.1. Dirichlet problems

Two different geometries are considered here. The first one is a circle of unit radius with two discretizations, and the second one is an ellipse with $a/b = 2{\cdot}00$.

4.1.1. Circle. The unit circle $x^2 + y^2 = 1$ is subjected to Dirichlet boundary conditions. In the present example, $\mathbf{N} = (x, y)$ and, from equation (26), $\phi_{\mathbf{N}}(x, y) = 4x^4 - 24x^2y^2 + 4y^4$. Note that both polynomials ϕ and $\phi_{\mathbf{N}}$ are of fourth order, while the Overhauser elements are cubic.

Two mesh discretizations have been considered, one with nodes at 10° intervals (36 nodes and elements) and the other one with nodes at 5° intervals (72 nodes and elements). Figure 2 shows the comparison between the exact and estimated errors for the two discretizations. The main feature of this graph is that the estimated errors follow the same trend of the exact errors for both discretizations. This graph also shows that (1) for each discretization, the estimator given by equation (4) overestimates the error; (2) as expected, the magnitude of the errors for the finer mesh (72 nodes) are smaller than the corresponding ones for the coarser mesh (36 nodes); (3) the difference between the estimated and exact errors are smaller for the finer mesh (72 nodes) than

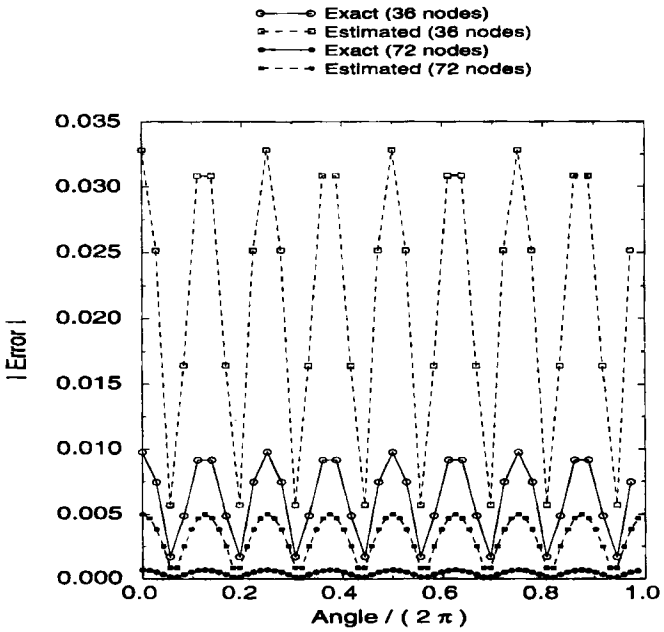

Figure 2. Exact (E) versus estimated ($\mathscr{E}$) errors for two mesh discretizations on the boundary of a circle with unit radius and Dirichlet boundary conditions

for the coarser one (36 nodes); and (4) the symmetry of the problem is captured by both the BEM solution (equation (1)) and the hypersingular BIE for the boundary error estimate (equation (4)).

4.1.2. Ellipse. Figure 3 shows a comparison between the exact and estimated errors for the ellipse $x^2 + y^2/(0{\cdot}5)^2 = 1{\cdot}0$ (i.e. $a/b = 2{\cdot}00$) discretized with 100 nodes. The errors estimated by equation (4) capture the trend of the actual error curve and predict reasonably well the magnitude of the actual errors.

4.2. Mixed boundary conditions

Again, the elliptical geometry with $a/b = 2$ is considered here, however, a coarser mesh discretization with 36 elements is employed. The mixed boundary conditions are Dirichlet on the top ($y \geqslant 0$), and Neumann on the bottom ($y < 0$) of the ellipse (equations (25) and (26), respectively). Two modelling strategies are presented below.

4.2.1. Simple modelling. The element connectivity for this example has followed the standard approach employed in the previous examples, i.e. nothing special is done at the $y = 0$ junctures of ∂B_d and ∂B_n. As the change in boundary conditions occurs at a smooth part of the boundary, this is appropriate. This same boundary value problem and discretization are used in the next two sections. Figure 4 shows a comparison between the exact and estimated errors. This is an interesting example, where the residual (represented by the estimated error curve in Figure 4) is approximately the same on the two parts of the boundary ($y \geqslant 0$ and $y < 0$), but the exact error is not. Nevertheless, the estimated error (obtained with equation (4)) is still reasonable because,

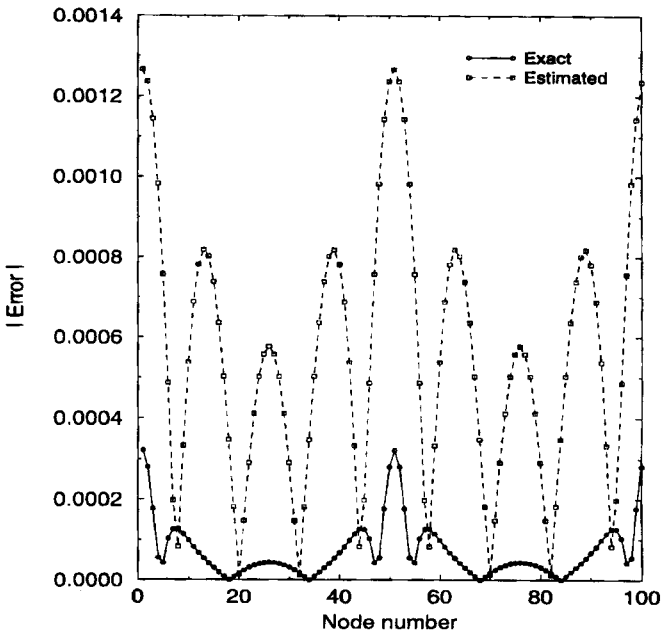

Figure 3. Exact (E) versus estimated ($\mathscr{E}$) errors for the elliptical geometry (100 nodes) with $a/b = 2$ and Dirichlet boundary conditions

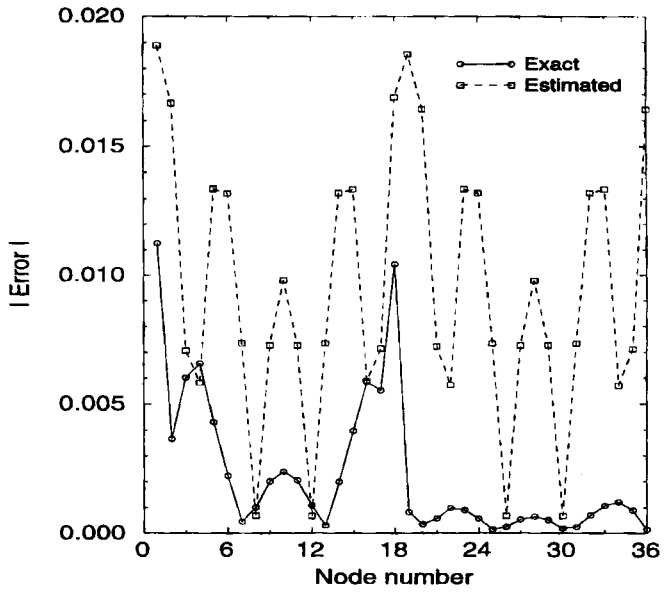

Figure 4. Exact (E) versus estimated ($\mathscr{E}$) errors for the elliptical geometry (36 nodes) with $a/b = 2$ and mixed boundary conditions

qualitatively, it indicates the global distribution and relative magnitude of the exact error for this coarse mesh discretization.

To illustrate the influence of the direction vector $\mathbf{D}$ and to justify our choice for $\mathbf{D} \equiv \mathbf{N}$ in equation (4), Figure 5 shows a comparison between the exact and estimated errors using $\mathbf{D} \equiv \mathbf{T}$ in

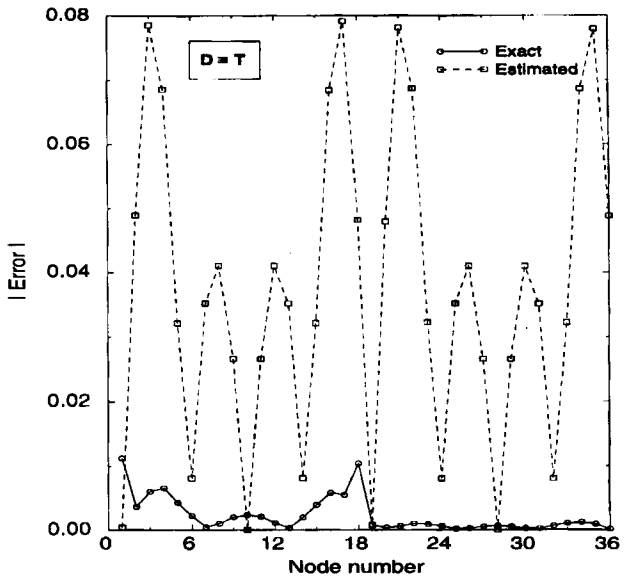

Figure 5. Exact (E) versus estimated ($\mathscr{E}$) errors for the elliptical geometry (36 nodes) with $a/b = 2$ and mixed boundary conditions. The estimated errors have been obtained with $\mathbf{D} \equiv \mathbf{T}$ in equation (4)

equation (4). Note that, in this case, the estimator seriously overestimates the errors at the $y = 0$ regions of the boundary (e.g. nodes 2. 19, 36). Moreover, the estimated and exact errors are out of phase between nodes 7–13 and 25–31. Therefore, a better prediction of the discretization errors is achieved with $\mathbf{D} \equiv \mathbf{N}$ than with $\mathbf{D} \equiv \mathbf{T}$ in equation (4).

4.2.2. 'Double node' modelling for change in boundary conditions. To introduce large errors, and therefore to test whether the error estimate $\mathscr{E}$ can respond to significant errors, the modelling near $y = 0$ was altered. Two extra nodes (37 and 38) have been added at the end of the nodal coordinates list. The 'double nodes' are 1 and 37, and 19 and 38. Nodes 1 and 19 are on the Dirichlet endpoints, and nodes 37 and 38 on the Neumann endpoints of the boundary. The element connectivity for this example is illustrated by Table I. Aside from being unnecessary, this procedure introduces errors by altering the Overhauser approximation to the geometry and functions in the neighbourhood of the $y = 0$ regions of the boundary. Figure 6 shows a comparison between the exact and estimated errors for this example. This graph shows that, as expected, the errors are concentrated on the double nodes, i.e. 1, 19, 37 and 38, and on their immediate neighbour nodes, while for the rest of the boundary the errors are much smaller. The error estimate given by equation (4) captures the trend of the actual errors, and gives a clear indication of serious problems in the 'double node' region.

4.3. Interior error estimates

As mentioned previously, interior error estimation is an important area of investigation. The purpose of this section is to examine the reliability of the formulation presented in Section 2.3. The calculation of the interior error makes use of previously calculated boundary error estimates (residual). Numerical results are presented for both the potential ϕ and its directional derivatives $\phi_{\mathbf{D}}$.

Table I. Element connectivity for 'double node' modelling using Overhauser elements.

El	El_Id	S_1	S_2	S_3	S_4
1	1	1	1	2	3
⋮	⋮	⋮	⋮	⋮	⋮
i	1	$i-1$	i	$i+1$	$i+2$
⋮	⋮	⋮	⋮	⋮	⋮
18	1	17	18	19	19
19	2	38	38	20	21
20	2	38	20	21	22
⋮	⋮	⋮	⋮	⋮	⋮
j	2	$j-1$	j	$j+1$	$j+2$
⋮	⋮	⋮	⋮	⋮	⋮
36	2	35	36	37	37

Note: El ≡ Element number; El_Id ≡ Element Identification (El_Id = 1 for Dirichlet and El_Id = 2 for Neumann boundary conditions); $1 < i < 18$; $20 < j < 36$

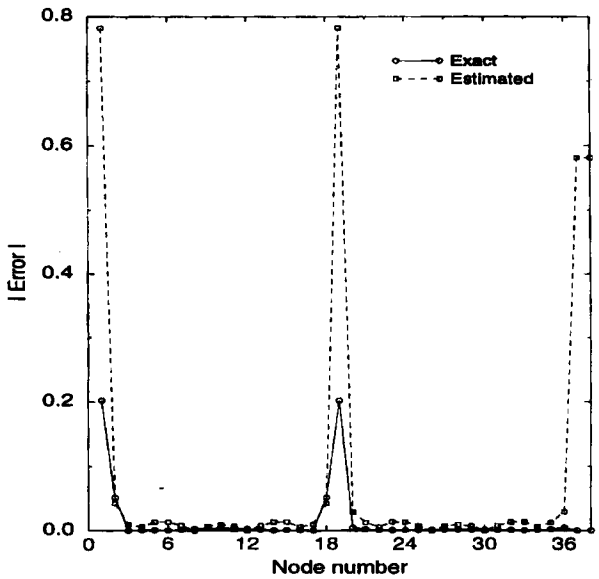

Figure 6. Exact (E) versus estimated ($\mathscr{E}$) errors for the elliptical geometry (38 nodes and 36 elements) using double node modelling for change in boundary conditions. Nodes 1 and 19 on the Dirichlet endpoints, and nodes 37 and 38 on the Neumann endpoints of the boundary

4.3.1. Error for $\phi(P)$, $P \in B$. Figure 7 shows a comparison between the exact and estimated errors for the potential on the circle $x^2 + y^2 = (0{\cdot}4)^2$ interior to the ellipse $x^2 + y^2/(0{\cdot}5)^2 = 1$. There are 36 interior points at 10° intervals. The graph in Figure 7 shows that (1) the estimator given by equation (15) overestimates the magnitude of the interior errors; (2) the estimator

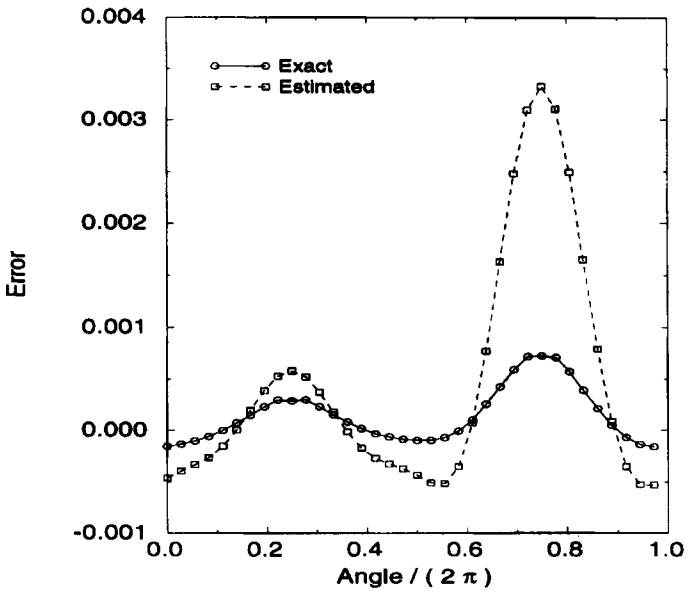

Figure 7. Exact (E_ϕ) versus estimated ($\hat{E}_\phi$) errors for the potential on the circle $x^2 + y^2 = (0{\cdot}4)^2$ interior to the ellipse $x^2 + y^2/(0{\cdot}5)^2 = 1$. There are 36 equally spaced interior points

provides a good prediction of the inflection points, shape and magnitude of the actual error curve; and (3) the difference between the exact and estimated errors is smaller on the top than on the bottom part of the circle. This last observation is quite reasonable, as Dirichlet boundary conditions are specified on the top of the ellipse, and the error is being calculated for the potential ϕ.

4.3.2. Error for $\phi_D(P)$, $P \in B$. Figure 8 shows a comparison between the exact and estimated errors for the directional derivatives of the potential on the same interior circle employed above. For each interior point, the direction **D** is the outward unit normal to the circle specified in a counter-clockwise sense. Therefore, from equation (26), $\phi_D = (4x^4 - 24x^2y^2 + 4y^4)/0{\cdot}4$. There are 36 interior points at 10° intervals. The graph in Figure 8 shows that (1) the estimator given by equation (18) overestimates the magnitude of the interior errors; and (2) the estimator provides a good prediction of the inflection points, shape and magnitude of the exact error curve. Note that there are two kinks in the exact error curve, one at the top and one at the bottom of the circle. This is probably due to the proximity of these points to the boundary. The distance between these points and the ellipse is 0·1 and the element length on the top or bottom of the ellipse is 0·1738. In this case, the techniques for interior point evaluation by Zhao *et al.*[47] could be employed for accurate computation of interior potential gradients.

It is interesting to note the similarity of the shape of the error curves in Figures 7 and 8, which have been obtained for two different quantities, i.e. the potential and its directional derivatives, respectively. This similarity is expected because, for the points on the circle $x^2 + y^2 = (0{\cdot}4)^2$, $\phi_D = 10\phi$, where ϕ is given by equation (25). As might be expected, the magnitude of the errors for the potential (see Figure 7) is less than those for its derivatives (see Figure 8). However, this is not always the case (see Reference 31).

Figure 9 shows a comparison between the exact and estimated errors for the directional derivatives of the potential on the straight segment $x = y$ from $x = -0{\cdot}35$ to $x = 0{\cdot}35$, which is

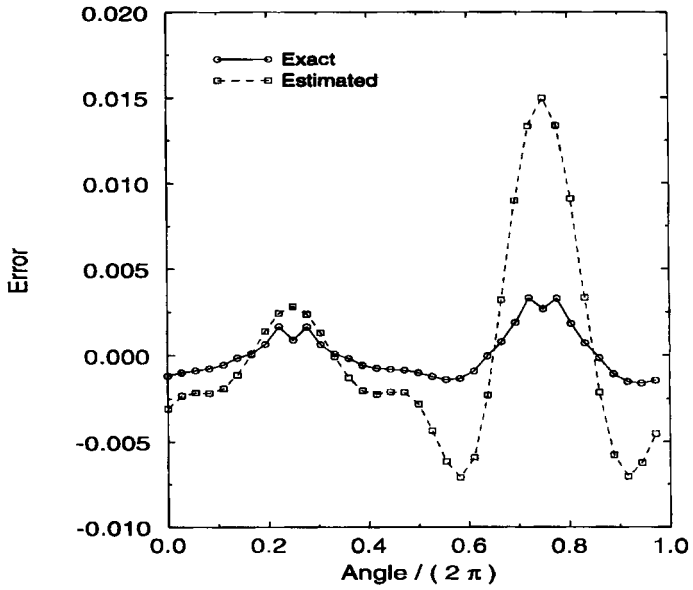

Figure 8. Exact ($E_{\phi D}$) versus estimated ($\mathscr{E}_{\phi D}$) errors for the directional derivatives of the potential on the circle $x^2 + y^2 = (0{\cdot}4)^2$ interior to the ellipse $x^2 + y^2/(0{\cdot}5)^2 = 1$. For each interior point, the direction **D** is the outward unit normal to the circle specified in a counter-clockwise sense. There are 36 equally spaced interior points

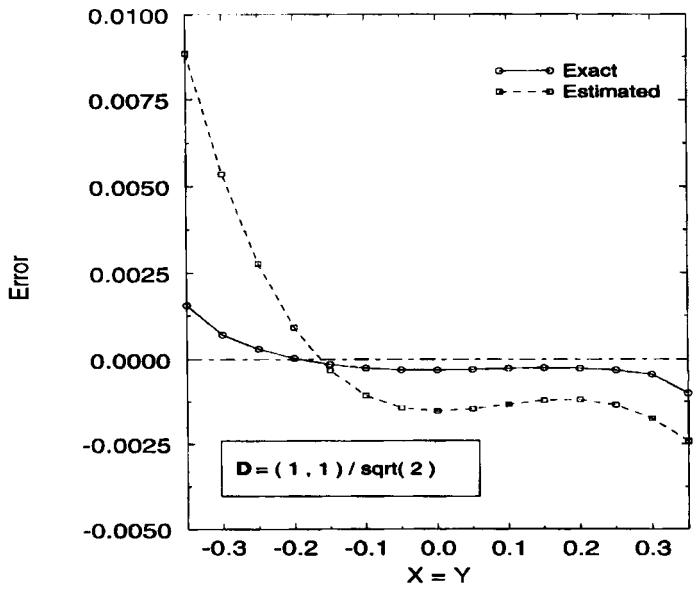

Figure 9. Exact ($E_{\phi D}$) versus estimated ($\mathscr{E}_{\phi D}$) errors for the directional derivatives of the potential on the straight segment $x = y$ from $x = -0{\cdot}35$ to $x = 0{\cdot}35$, which is interior to the ellipse $x^2 + y^2/(0{\cdot}5)^2 = 1$. There are 15 equally spaced interior points

interior to the ellipse $x^2 + y^2/0{\cdot}5^2 = 1$. The derivatives are evaluated in the direction $\mathbf{D} = (1, 1)/\sqrt{2}$. Therefore, from equation (26), $\phi_{\mathbf{D}} = -16x^3/\sqrt{2}$. There are 15 equally spaced interior points, one at each 0·05 length interval. For this example, the estimator given by equation (18) once again gives a good prediction for the shape and magnitude of the actual errors.

4.4. *Verification of the 'symmetry' of the method with respect to equations* (1) *and* (3)

The 'symmetry' of the two BIEs, one for solution of the problem and one for error estimation, has been discussed in Section 2.4 (Remark 2). To support this argument, an example with Dirichlet boundary conditions is presented here. It is worth mentioning that there is a rationale for solving Dirichlet problems using the hypersingular BIE. Ingber and Mondy[32] have pointed out that a stable second kind integral equation is obtained by employing a hypersingular equation for this type of problem, while the standard boundary integral formulation leads to a potentially unstable first kind integral.

Figure 10 shows the exact versus estimated errors for the elliptical geometry (36 nodes) with $a/b = 2$ and Dirichlet boundary conditions. The boundary value problem has been solved by equation (3), and the errors have been estimated by equation (20). In this example the estimator underestimates the error. However, the shape of the actual error curve is well predicted. This can be easily verified by normalizing both the exact and the estimated errors with respect to the maximum error for each quantity. This is shown in Figure 11. The trend of this graph shows that the normalized estimated errors overestimate the normalized actual errors for this example.

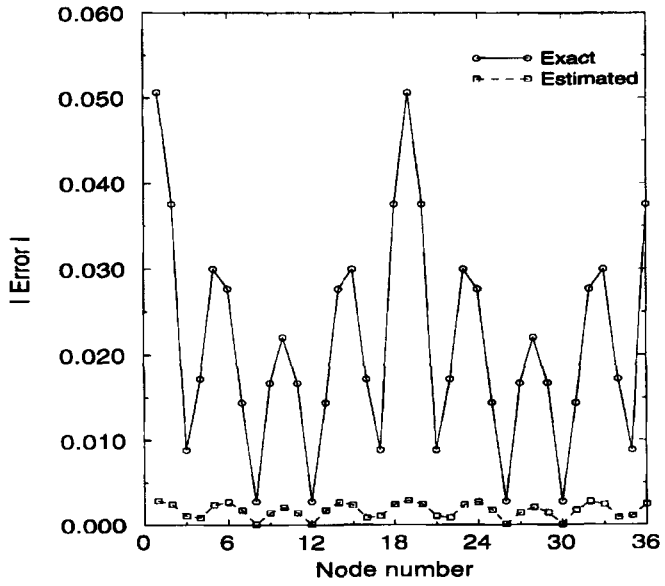

Figure 10. Exact (E) versus estimated ($\mathscr{E}$) errors for the elliptical geometry (36 nodes) with $a/b = 2$, and Dirichlet boundary conditions. Equation (20) has been used for error estimation

4.5. *Generic example: L-shaped object*

The last example, extracted from Reference 35, is reasonably representative of geometry and boundary conditions that arise in practice, and it does not have an analytical solution. The geometry is shown in Figure 12. The left verticle face (at $x = 0$) of the object is maintained at $\phi = 1000$ units, while the right vertical face (at $x = 120$) is forced to be at $\phi = 0$ units. All the other boundaries are perfectly insulated, i.e. $\phi_n = 0$ units.

The discretization adopted for the L-shaped object consists of 97 nodes (92 geometrically distinct nodes and 5 double nodes at the corners) and 92 Overhauser elements. Table II compares

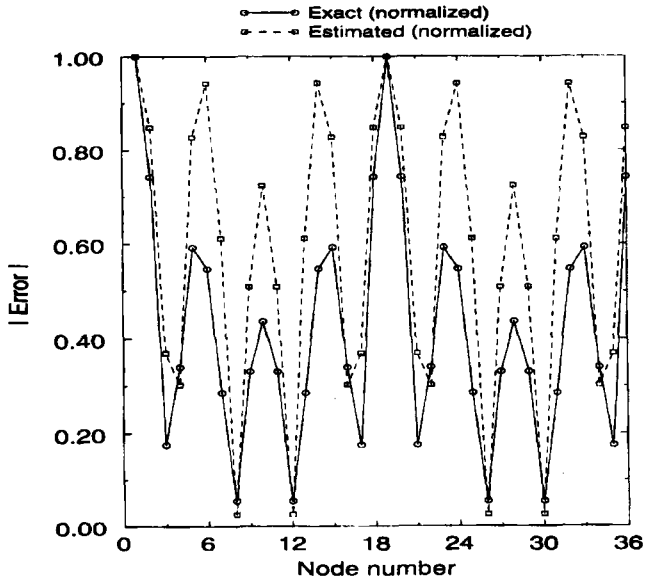

Figure 11. Exact (E) versus estimated ($\mathscr{E}$) normalized errors for the elliptical geometry (36 nodes) with $a/b = 2$ and Dirichlet boundary conditions. Equation (20) has been used for error estimation

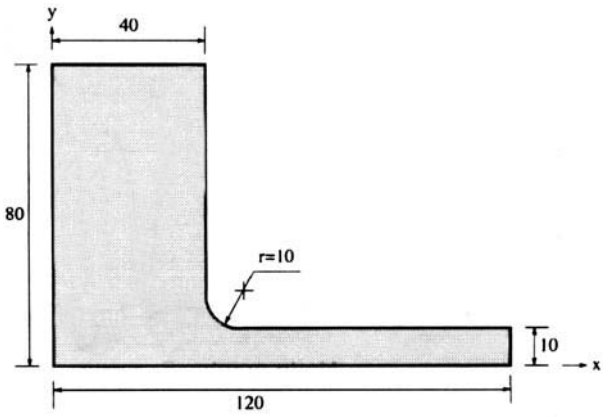

Figure 12. L-shaped object

the results obtained with the present implementation and those reported in Reference 35 for the symmetric Galerkin boundary element analysis with analytical evaluation of singular integrals. The discretization used in Reference 35 consists of 92 distinct nodes and 46 isoparametric quadratic elements. The present discretization and the one in Reference 35 have the same set of nodal points in the boundary element mesh. From Table II, it is observed that a good agreement between the two boundary element solutions is achieved. As noted in Section 2.4 (Remark 2), it would be very interesting to estimate the error in a symmetric Galerkin context using the ideas presented in this paper.

Table II. Response of L-shaped object

	Sample point		Overhauser		Galerkin BEM	
Node	x	y	ϕ	ϕ_n	ϕ	ϕ_n
6	25·0	0·0	926·14	0·0	926·10	0·0
18	85·0	0·0	379·50	0·0	379·37	0·0
27	120·0	3·33	0·0	− 10·827	0·0	− 10·841
29	120·0	6·67	0·0	− 10·827	0·0	− 10·841
34	105·0	10·0	162·64	0·0	162·57	0·0
45	55·0	10·0	705·37	0·0	705·07	0·0
49	46·17	10·76	814·09	0·0	813·88	0·0
51	42·93	12·93	860·38	0·0	860·34	0·0
58	40·0	27·5	945·43	0·0	945·45	0·0
66	40·0	65·0	984·94	0·0	984·93	0·0
72	25·0	80·0	989·41	0·0	989·40	0·0
82	0·0	55·0	1000·0	0·748	1000·0	0·748
92	0·0	5·0	1000·0	2·537	1000·0	2·536

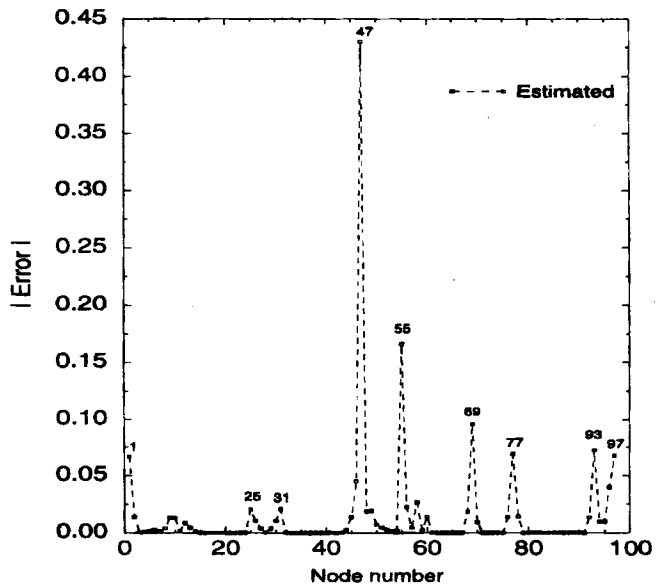

Figure 13. Estimated ($\mathscr{E}$) errors for the L-shaped domain (97 nodes and 92 elements) with mixed boundary conditions. The numbers above the points denote nodal numbers

Figure 13 shows the estimated errors for the L-shaped object discretized with 97 nodes and 92 Overhauser elements. The two more pronounced peaks are at nodes 47 ($\mathbf{n} = (0, 1)$) and 55 ($\mathbf{n} = (1, 0)$), which correspond to the endpoints of the circular arc. These error peaks are expected because regions with high curvature are expected to have a large error. Moreover, the error at node 47 is bigger than the error at node 55. This too is reasonable, as node 47 is located on the long thin part of the L-shaped object. There are smaller peaks at nodes 1, 25, 31, 69 and 77. These are the corner nodes. The double nodes, corresponding to each of these corner nodes are located at the end of nodal list, i.e. nodes 93 to 97. There is a perturbation on the error curve involving nodes 8–14. This is an interesting phenomenon. It is probably due to the influence of change of curvature on the part of the boundary which is immediately above the segment from nodes 8–14. Finally, this example shows that the estimator given by equation (20) also gives a very good indication of the actual error for this complicated problem.

5. CONCLUSIONS AND EXTENSIONS

This work indicates that the combination of the standard and hypersingular integral equations provides a good basis for evaluating the discretization error in boundary element analysis. The present error estimation method is of the residual type and consists of substituting the approximate boundary element solution into the corresponding hypersingular integral equation. The boundary error estimates can then be employed for evaluating the interior error estimates for the potential and the directional derivatives of the potential. As pointed out previously, the argument which led to equation (4) is 'symmetric', in that the role of the two equations (1) and (3) can be reversed. This property is essential for estimating the error using a symmetric-Galerkin BEM. Moreover, the fact that the error estimates have an explicit form is potentially advantageous for mathematical analysis (see Section 2.2.1 and References 48–50).

The error estimation procedure has been presented using a scalar field. Nevertheless, this work naturally extends to vector field problems (see Appendix). For example, using the BEM formulation for linear elasticity[51] together with the traction BIE (e.g. see Reference 19), and following the methodology developed herein, one can obtain expressions for the error estimates which are analogous to equations (4), (15) and (18). However, in this vector field case, the boundary error is a vector, the interior displacement error is also a vector, and the interior stress error is a tensor. These are basic forms for the errors, and if desired, an appropriate error norm can be obtained from the error components. It is worth investigating if the same principles for error estimation also hold for equations other than elliptic, e.g. parabolic and hyperbolic. This is a subject for future work.

Extensive numerical testing of the error estimates has been carried out for the two-dimensional Laplace equation. The influence of several factors have been investigated, such as geometry of the body, boundary conditions and discretization. The numerical results show that both the boundary and interior error estimates provide a remarkably faithful tracking of the exact error curve and a reasonable estimate of the magnitude of the exact error. Preliminary and encouraging results have also been obtained to validate the 'symmetry' argument for error estimation.

The residual type error estimation method presented in this paper is intrinsic to the BEM technique. It is applicable to any boundary integral formulation, can be readily extended to three-dimensional problems (see Section 2.4), and allows a 'pointwise' estimation of the discretization error. With respect to this last point, it is worth mentioning that in many design problems, one is interested in assessing the error at particularly critical parts of the boundary. Therefore, the error $\mathscr{E}(P)$ could be evaluated just at points in these specific regions of interest, rather than at all boundary nodes.

An integration over the entire boundary is required to evaluate $\mathscr{E}(P)$ (see equations (4) and (20)) for every P. Thus, the possibility of reducing the computational cost by neglecting 'far-field' integrals should be investigated. There are additional interesting topics for future investigation, for example, development of error estimates with a continuous limit to the boundary, the use of equation (8) to obtain an error estimate which might be better than the residual given by equation (4), error estimation using a symmetric-Galerkin BEM formulation, sensitivity analysis of the error estimates and extension of the error estimates to non-linear and vector field problems. The present work also offers room for extension to other applications such as sensitivity analysis, fracture mechanics and solution adaptive techniques. In what follows, brief explanations, concerning these three applications, are given.

The explicit form of the error estimates (equations (4), (15) and (18)) allows their direct use in sensitivity analysis. Thus, analytical expressions for the sensitivities of the errors on the boundary and in the interior can be readily derived, as shown by Paulino *et al.*[31] Evaluation of the sensitivity of the errors is important in applications such as shape optimization using adaptive refinement.[52] Information on sensitivity analysis and optimization in computational mechanics can be found in the books by Haug *et al.*,[53] and Haftka and Gürdal.[54]

A very interesting subject for future research is the extension of the present method to crack problems, which includes error estimation in fracture mechanics (see, for example, Reference 55). In one technique, both the hypersingular integral equation and the standard BEM equation are already employed on the crack surface to solve the problem.[19,56] Therefore, there is no longer an additional equation available for the error estimation. One possibility, however, is to use the hypersingular equation, with the direction $\mathbf{D}$ being taken tangent to the crack surface.

As the error estimation method appears to provide a reliable tracking of the actual error, it should be highly suitable for a self-adaptive procedure. A natural extension of this work consists of using the local errors as the driving parameters of an adaptive mesh refinement scheme, e.g. h-refinement. While the boundary errors $\mathscr{E}$ give information about the error distribution, an automatic adaptive refinement gives results within a specified accuracy.

The range of application of the new error estimates is potentially broad. Use of the techniques presented in this paper could contribute towards a reliable and automated environment in computational mechanics (e.g. see Reference 57) employing BIE techniques.

ACKNOWLEDGEMENTS

This work was supported by the Applied Mathematical Sciences Subprogram, Office of Basic Energy Sciences, and the GO-NII project, U.S. Department of Energy, under contract DE-AC05-84OR21400 with Martin Marietta Energy Systems Inc. The first author would like to acknowledge partial financial support provided by the CNPq Brazilian Agency. V. Zarikian's work was part of the Research Experiences for Undergraduates Program, funded by National Science Foundation and the University of Tennessee Science Alliance.

APPENDIX: ERROR ESTIMATION METHOD IN ELASTICITY

A general methodology for error estimation has been presented in Section 2. Following this procedure, a formulation is presented for evaluating the discretization error in elasticity problems. This formulation illustrates the general scheme to be adopted for error estimation in vector field problems. The definition of singular and hypersingular integrals is once again taken as a *limit-to-the-boundary*.[18,19] In the interest of brevity, only the main equations are given below.

The standard direct BEM formulation for linear elasticity,[51] in the absence of body forces, can be written as

$$u_j(P) + \int_{\partial B} u_i(Q) T_{ij}(P,Q)\,\mathrm{d}s_Q = \int_{\partial B} \tau_i(Q) U_{ij}(P,Q)\,\mathrm{d}s_Q \tag{27}$$

where u_i and τ_i are the displacement and traction vectors, respectively, and T_{ij} and U_{ij} are the usual Kelvin kernels.

For a linear elastic isotropic body, the internal stresses can be obtained by differentiating the displacements at internal points (equation (27)) and introducing the displacement derivatives into the stress–strain relationship

$$\sigma_{ij}(P) = \mu(u_{i,j} + u_{j,i}) + \lambda u_{k,k}\delta_{ij} \tag{28}$$

where λ and μ are the Lamé constants for the material, and δ_{ij} is the Kronecker delta. After some algebra, the stress BIE can be written in a compact form as

$$\sigma_{ij}(P) = -\int_{\partial B} u_k(Q) S_{kij}(P,Q)\,\mathrm{d}s_Q + \int_{\partial B} \tau_k(Q)\, D_{kij}(P,Q)\,\mathrm{d}s_Q \tag{29}$$

where the differentiated Kelvin kernels S_{kij} and D_{kij} can be found in many books on BEM, e.g. Reference 30.

The traction BIE can be obtained from equation (29) as follows:

$$\begin{aligned}\tau_i(P) &= \sigma_{ij} N_j \\ &= \left[-\int_{\partial B} u_k(Q) S_{kij}(P,Q)\,\mathrm{d}s_Q + \int_{\partial B} \tau_k(Q) D_{kij}(P,Q)\,\mathrm{d}s_Q \right] N_j\end{aligned} \tag{30}$$

where $\mathbf{N} = \mathbf{n}(P)$ ($\mathbf{N} = N_i \mathbf{e}_i$ and $\mathbf{e}_i$ ($i = 1,2,3$) are global Cartesian unit vectors).

A.1. Boundary error estimate

Assume that a particular problem has been solved using equation (27), resulting in approximate solutions

$$\tilde{\mathbf{u}} \quad \text{and} \quad \tilde{\boldsymbol{\tau}}$$

for the unknown boundary values of displacements and tractions, respectively. Although these functions have been determined to satisfy equation (27), they are not necessarily consistent with equation (30).

The proposed error indicator vector $\mathscr{E}(P)$ is defined as the residual which arises when the approximate solution is substituted into equation (30), i.e. $\mathscr{E}(P)$ is the *hypersingular residual*. Thus,

$$\mathscr{E}_i(P) = -\tilde{\tau}_i(P) - N_j \int_{\widetilde{\partial B}} \tilde{u}_k(Q) S_{kij}(P,Q)\,\mathrm{d}s_Q + N_j \int_{\widetilde{\partial B}} \tilde{\tau}_k(Q) D_{kij}(P,Q)\,\mathrm{d}s_Q \tag{31}$$

This equation is analogous to equation (4), except that the error in equation (4) is a scalar quantity, and the error in equation (31) is a vector quantity.

A.2. Error estimate for $u(P), P \in B$

Following the ideas presented in Section 2, one arrives at the BIE for the error on the displacement at internal points

$$\mathscr{E}_{j_{(u)}}(P) = -\int_{\partial B} \mathscr{E}_{i_{(u)}}(Q) T_{ij}(P,Q)\,\mathrm{d}s_Q + \int_{\partial B} \mathscr{E}_{i_{(\tau)}}(Q) U_{ij}(P,Q)\,\mathrm{d}s_Q \tag{32}$$

where for Dirichlet portions of the boundary, $\mathscr{E}_{i_{(\tau)}}(Q) \equiv \mathscr{E}_i(P)$, and *assume* (see comments in Remark 3, Section 2.4)

$$\mathscr{E}_{i_{(u)}}(Q) \equiv 0 \tag{33}$$

Similarly, for Neumann portions of the boundary, $\mathscr{E}_{i_{(u)}}(Q) \equiv \mathscr{E}_i(P)$, and *assume*

$$\mathscr{E}_{i_{(\tau)}}(Q) \equiv 0 \tag{34}$$

Equation (32) is analogous to equation (15). Note, however, that the error in equation (32) is now a vector quantity.

A.3. Error estimate for $\sigma(P), P \in B$

Using the above framework for error analysis in elasticity problems and the ideas presented in Section 2, one arrives at the BIE for the error on the stress tensor at internal points

$$\mathscr{E}_{ij_{(\sigma)}}(P) = -\int_{\partial B} \mathscr{E}_{k_{(u)}}(Q) S_{kij}(P,Q)\,\mathrm{d}s_Q + \int_{\partial B} \mathscr{E}_{k_{(\tau)}}(Q) D_{kij}(P,Q)\,\mathrm{d}s_Q \tag{35}$$

Also here, $\mathscr{E}_{i_{(\tau)}}(Q) \equiv \mathscr{E}_i(P)$ and $\mathscr{E}_{i_{(u)}}(Q) \equiv \mathscr{E}_i(P)$ for Dirichlet and Neumann portions of the boundary, respectively. Moreover, the assumptions on equations (33) and (34) are also employed in this case. Equation (35) is analogous to equation (18). Note, however, that the error in equation (35) is now a second-order tensor quantity.

The above formulation for the interior error estimates for $\mathbf{u}(P)$ and $\boldsymbol{\sigma}(P)$ is not continuous to the boundary. However, continuity at the boundary can be achieved at the expense of additional computations, as explained in Remark 3 of Section 2.4.

REFERENCES

1. E. Kita and N. Kamiya, 'Recent studies on adaptive boundary element methods', *Adv. Eng. Software*, **19**, 21–32 (1994) (cites 82 references).
2. C. A. Brebbia and M. H. Aliabadi (eds.), *Adaptive Finite and Boundary Element Methods*, Computational Mechanics Publications, Southampton, and Elsevier Applied Science, London, 1993.
3. I. Babuška, O. C. Zienkiewicz, J. Gago and E. R. de A. Oliveira (eds.), *Accuracy Estimates and Adaptive Refinements in Finite Element Computations*, Wiley, Chichester, 1986.
4. A. K. Noor and I. Babuška, 'Quality assessment and control of finite element solutions', *Finite Elements Anal. Des.*, **3**, 1–26 (1987) (cites 196 references).
5. J. T. Oden and L. Demkowicz, 'Advances in adaptive improvements—A survey of adaptive finite element methods in computational mechanics', in A. K. Noor and J. T. Oden (eds.), *State-Of-The-Art Surveys On Computational Mechanics*, The American Society of Mechanical Engineers (ASME), New York, Chapter 13, pp. 441–467 (1989) (cites 184 references).
6. T. Strouboulis and K. A. Haque, 'Recent experiences with error estimation and adaptivity, Part I: Review of error estimators for scalar elliptic problems', *Comp. Methods Appl. Mech. Eng.*, **97**, 399–436 (1992).
7. T. Strouboulis and K. A. Haque, 'Recent experiences with error estimation and adaptivity, Part II: Error estimation for h-adaptive approximations on grids of triangles and quadrilaterals', *Comp. Methods Appl. Mech. Eng.*, **100**, 359–430 (1992).
8. I. Babuška and M. Suri, 'The P and H-P versions of the finite element method, basic principles and properties', *SIAM Rev.*, **36**, 578–632 (1994).

9. J. Mackerle, 'Mesh generation and refinement for FEM and BEM—A bibliography (1990–1993)', *Finite Elements Anal. Des.*, **15**, 177–188 (1993) (cites 272 references in FEM and 23 in BEM).
10. I. Babuška, J. Chandra and J. E. Flaherty (eds.), *Adaptive Computational Methods for Partial Differential Equations*, SIAM (Society for Industrial and Applied Mathematics), Philadelphia, 1983.
11. D. W. Kelly, R. J. Mills, J. A. Reizes and A. D. Miller, '*A posteriori* estimates of the solution error caused by discretization in the finite element, finite difference and boundary element methods', *Int. j. numer. methods eng.*, **24**, 1921–1939 (1987).
12. O. C. Zienkiewicz and R. L. Taylor, *The Finite Element Method, Vol. 1: Basic Formulation and Linear Problems*, McGraw-Hill, London, 1989.
13. O. C. Zienkiewicz and J. Z. Zhu, 'The superconvergent patch recovery and *a posteriori* error estimates. Part 1: The recovery technique', *Int. j. numer. methods. eng.*, **33**, 1331–1364 (1992).
14. O. C. Zienkiewicz and J. Z. Zhu, 'The superconvergent patch recovery and *a posteriori* error estimates. Part 2: Error estimates and adaptivity', *Int. j. numer. methods eng.*, **33**, 1365–1382 (1992).
15. O. C. Zienkiewicz and J. Z. Zhu, 'The SPR recovery and boundaries', *Int. j. numer. methods eng.*, **37**, 3195–3196 (1994).
16. B. Szabó and I. Babuška, *Finite Element Analysis*, Wiley, New York, U.S.A., 1991.
17. M. Guiggiani, 'Error indicators for adaptive mesh refinement in the boundary element method—A new approach', *Int. j. numer. methods eng.*, **29**, 1247–1269 (1990).
18. L. J. Gray, 'Boundary element method for regions with thin internal cavities', *Eng. Anal. Boundary Elements*, **6**, 180–184 (1989).
19. L. J. Gray, L. F. Matha and A. R. Ingraffea, 'Hypersingular integrals in boundary element fracture analysis', *Int. j. numer. methods eng.*, **29**, 1135–1158 (1990).
20. L. J. Gray and L. L. Manne, 'Hypersingular integrals at a corner', *Eng. Anal. Boundary Elements*, **11**, 327–334 (1993).
21. G. Krishnasamy, F. J. Rizzo and T. J. Rudolphi, 'Hypersingular Boundary integral Equations: Their occurrence, interpretation, regularization and computation', in P. K. Banerjee and S. Kobayashi (eds.), *Developments in Boundary Element Methods*, Elsevier Applied Science, London and New York, 1992, Vol. 7, Chapter 6, pp. 207–252.
22. M. Guiggiani, G. Kriahnasamy, T. J. Rudolphi and F. J. Rizzo, 'A general algorithm for the numerical solution of hypersingular boundary integral equations', *ASME J. Appl. Mech.*, **59**, 604–614 (1992).
23. D. Rosen and D. E. Cormack, 'Analysis and evaluation of singular integrals by the invariant imbedding approach', *Int. j. numer. methods eng.*, **35**, 563–587 (1992).
24. D. Rosen and D. E. Cormack, 'Singular and near singular integrals in the BEM: A global approach', *SIAM J. Appl. Math.*, **53**, 340–357 (1993).
25. E. D. Lutz and L. J. Gray, 'Analytic evaluation of singular boundary integrals without CPV', *Commun. numer. methods eng.*, **9**, 909–915 (1993).
26. L. J. Gray, 'Symbolic computation of hypersingular boundary integrals', in J. H. Kane, G. Maier, N. Tosaka and S. N. Atluri (eds.), *Advances in Boundary Element Techniques*, Springer, Berlin, Heidelberg, 1993, Chapter 8, pp. 157–172.
27. P. Parreira and Y. F. Dong, 'Adaptive hierarchical boundary elements', *Adv. Eng., Software*, **15**, 249–259 (1992).
28. P. Partridge, C. A. Brebbia and L. C. Wrobel, *The Dual Reciprocity Boundary Element Method*, Computational Mechanics Publications, Southampton and Elsevier Applied Science, London, 1991.
29. X. Wei, A. Chandra, L.-J. Leu and S. Mukherjee, 'Shape optimization in elasticity and elasto-viscoplasticity by the boundary element method', *Int. J. Solids Struct.*, **31**, 533–550 (1994).
30. A. Chandra and S. Mukherjee, *Boundary Element Methods in Manufacturing*, Oxford University Press, 1996.
31. G. H. Paulino, L. J. Gray and V. Zarikian, *A Posteriori Pointwise Error Estimates for the Boundary Element Method*, Technical Memorandum ORNL/TM-12820, Oak Ridge National Laboratory, Oak Ridge, TN 37831, U.S.A. 1994.
32. M. S. Ingber and L. A. Mondy, 'Direct second kind boundary integral formulation for Stokes flow problems', *Comput. Mech.*, **11**, 11–27 (1993).
33. F. Hartmann, C. Katz and B. Protopsaltis, 'Boundary elements and symmetry', *Ing. Archiv*, **55**, 440–449 (1985).
34. G. Maier, M. Diligenti and A. Carini, 'On symmetrization in boundary element elastic and elastoplastic analysis', in G. Kuhn and H. Mang (eds.), *Discretization Methods in Structural Mechanics*, Springer, Berlin, 1990, pp. 191–200.
35. C. Balakrishna, L. J. Gray and J. H. Kane, 'Efficient analytical integration of symmetric Galerkin boundary integrals over curved elements: Thermal conduction formulation', *Comp. Methods Appl. Mech. Eng.*, **111**, 335–355 (1994).
36. D.-H. Yu, 'Self-adaptive boundary element methods', *Zeitshrift für angewandte Mathematik und Mechanik*, **68**(5), T435–T437 (1988).
37. D.-H. Yu, 'Mathematical foundation of adaptive boundary element methods', *Comp. Methods Appl. Mech. Eng.*, **91**, 1237–1243 (1991).
38. W. L. Wendland and D.-H. Yu, '*A-posteriori* local error estimates of boundary element methods with some pseudo-differential equation on closed curves', *J. Comput. Math.*, **10**, 273–289 (1992).
39. E. Rank, 'Adaptive h-, p- and hp-versions for boundary integral element methods', *Int. j. numer. methods eng.*, **28**, 1335–1349 (1989).
40. W. Sun and N. G. Zamani, 'An adaptive h-r boundary element algorithm for the Laplace equation', *Int. j. numer. methods eng.*, **33**, 537–552 (1992).
41. K. Abe, 'A new residue and nodal error evaluation in *h*-adaptive boundary element method', *Adv. Eng. Software*, **15**, 231–239 (1992).

42. M. S. Ingber and A. K. Mitra, 'Grid redistribution based on measurable error indicators for the direct boundary element method', *Eng. Anal. Boundary Elements*, **9**, 13–19 (1992).
43. C. V. Camp and G. S. Gipson, 'Overhauser elements in Boundary element analysis', *Math. Comp. Modelling*, **15**, 59–69 (1991).
44. G. Krishnasamy, F. J. Rizzo and T. J. Rudolphi, 'Continuity requirements for density functions in the boundary integral equation method', *Comput. Mech.*, **9**, 267–284 (1992).
45. G. H. Paulino, 'Novel formulations of the boundary element method for fracture mechanics and error estimation', *Ph.D. Dissertation*, Cornell University, Ithaca, NY, U.S.A., 1995.
46. V. Zarikian, L. J. Gray and G. H. Paulino, 'Pointwise error estimates for boundary element calculations', in C. A. Brebbia and A. J. Kassab (eds.), *Boundary Element Technology IX*, Computational Mechanics Publications, Southampton and Boston, 1994, pp. 253–260.
47. C. Zhao, M. Ailor and L. J. Gray, 'Interior point evaluation in the boundary element method', *Eng. Anal. Boundary Elements*, **13**, 201–208 (1994).
48. N. Ghosh, 'On the convergence of the boundary element method', *Ph.D. Dissertation*, Cornell University, Ithaca, NY., U.S.A., 1982.
49. C. Johnson, *Numerical Solution of Partial Differential Equations by the Finite Element Method*, Cambridge University Press, New York, 1987.
50. I. H. Sloan, 'Error analysis of boundary integral methods', *Acta Numerica*, 287–339 (1992).
51. F. J. Rizzo, 'An integral equation approach to boundary value problems of classical elastostatics', *Quart. Appl. Math.*, **25**, 83–95 (1967).
52. G. Bugeda and J. Oliver, 'A general methodology for structural shape optimization problems using automatic adaptive remeshing', *Int. j. numer. methods eng.*, **36**, 3161–3185 (1993).
53. E. J. Haug, K. K. Choi and V. Komkov, *Design Sensitivity Analysis of Structural Systems*, Academic Press, Orlando, FL, 1986.
54. R. T. Haftka and Z. Gürdal, *Elements of Structural Optimization*, 3rd. revised and expanded edition, Kluwer Academic Publishers, Dordrecht, 1992.
55. K. Jayaswal and I. R. Grosse, 'Finite element error estimation for crack tip singular elements', *Finite Elements Anal. Des.*, **14**, 17–35 (1993).
56. L. J. Gray and C. S. Soucie, 'A Hermite interpolation algorithm for hypersingular boundary integrals', *Int. j. numer. methods eng.*, **36**, 2357–2367 (1993).
57. W. W. Tworzydlo and J. T. Oden, 'Towards an automated environment in computational mechanics', *Comp. Methods Appl. Mech. Eng.*, **104**, 87–143 (1993).